

## Design, application, and power performance analyses of a micro wind turbine

Hayati MAMUR\*

Department of Electrical-Electronics Engineering, Faculty of Engineering, Çankırı Karatekin University,  
Çankırı, Turkey

Received: 19.01.2014

Accepted/Published Online: 16.08.2014

Printed: 30.11.2015

**Abstract:** In this study, design, implementation, and power performance analyses of a micro wind turbine (MWT) system are presented. An original permanent magnet synchronous generator (PMSG) that reduced cogging torque was employed as a generator in the MWT. A novel blade form offering better performance at low wind speeds was also utilized for the MWT blades. Power performance analyses of the MWT were carried out for different wind regimes by truck testing. Performance coefficient, cut-in, and cut-out of the MWT were determined as 27.7%, 2.7 m/s, and 20 m/s at the end of the truck testing, respectively. Moreover, a new supervisory control and data acquisition (SCADA) program based on a programmable logic controller was written to measure the electrical power of the MWT, and hence the analyses of the MWT were easily fulfilled through the SCADA.

**Key words:** Energy, renewable energy, wind energy, micro wind turbine, truck test

### 1. Introduction

Recently, wind energy has become one of the most rapidly increasing renewable energy resources. One of the methods for converting electrical energy into wind energy is to use wind turbines (WTs). WTs are manufactured in different sizes and powers [1]. According to the IEC 61400-2 standard of the International Electrotechnical Commission (IEC), WTs are divided into 2 classes: small WTs (SWTs), having a rotor-swept area of 200 m<sup>2</sup> or less, and large WTs (LWTs), with a rotor-swept area larger than 200 m<sup>2</sup>. According to the Small and Medium Wind UK Market Report 2013 (<http://www.renewableuk.com/en/publications/index.cfm/Small-and-Medium-Wind-UK-Market-Report-2013>), commercially manufactured SWTs are analyzed in 3 classes: micro WTs (MWTs), SWTs, and small-medium WTs (SMWTs).

On account of the installation costs of MWTs being less than those of other renewable energy resources, MWTs are generally more preferred in places such as cottages, pastures, bungalows, chalets, barns, fields, and recreational areas, where there is no electricity grid. Lately, MWTs have been more widely utilized as an alternative energy resource in the United States, China, and European Union countries. It is also seen that Turkey has the potential of usage of MWTs because the sea coasts of Turkey have average wind speeds of 4.5 to 10 m/s [2]. Considering also the density of settlements along the Black Sea coast of Turkey, MWTs become much more important renewable energy resources [3]. MWTs can be manufactured in many different forms. These are off-grid, on-grid, vertical axis (VAWT), and horizontal axis (HAWT). Their power is between 0 and 1.5 kW, the annual electricity production (AEP) capacity is below 1 GWh/year, and the tower height is about 10–18 m [4].

\*Correspondence: [hmamur@karatekin.edu.tr](mailto:hmamur@karatekin.edu.tr)

A MWT basically consists of a generator, 3–5 blades, a tail, a tower, and electrical equipment. Induction generators (IGs) and permanent magnet synchronous generators (PMSGs) are widely used as generators in MWTs [5,6]. PMSGs give variable voltage and frequency due to variable speeds [7]. In recent times, PMSGs are more preferred than IGs, since they have small dimensions, high efficiency, and high power density and are direct-drive [8].

PMSGs are called internal or external rotors as regards the placement of the magnets used in the rotor [9]. The PMSGs with external rotors have less weight and lower cost than PMSGs with internal rotors. However, the PMSGs with internal rotors give higher torque and power output. Cost, weight, size, torque, and obtained power influence the type of PMSG to be used for a MWT application. It is also preferred that the PMSG have mechanically lower rotational speed. This means that the PMSG has a higher number of poles [8]. Magnets used in PMSGs have a major impact on the performance of PMSGs. Commercially available magnets such as ceramic or polymer-bonded neodymium-iron-boron are utilized [10]. Reducing cogging torque, obtaining higher torque, minimizing torque changes, boosting efficiency, and enhancing flux density of the groove-pole structure play important roles in PMSGs. One of the methods of cogging torque reduction is based on the configuration of the stator slot number and the number of pole pairs. This results in the use of the fractional-slot stator winding [11–14].

Taking into consideration the blade structures of MWTs, the first blades employed in MWTs had a flat-blade form used in windmills. Afterwards, a slightly convex curved blade form was utilized in multibladed wind pumps, called American-type windmills. This blade form was the most commonly utilized until the 1950s. After the 1950s, blades formed in an airplane blade structure were begun to be used in parallel with the developments in flight aerodynamics [15,16]. In today's technology, the optimized forms of the blades have been utilized [17]. Pathike et al. [18] achieved higher torque in MWTs at low wind speeds on the basis of the blade element momentum theory with a new blade form, developed previously as the FD2.7-500 and modified. They achieved 27% greater efficiency than commercially available blades. Rolak et al. [19] used their own blade form in their designed MWT. Selig and McGranahan [20,21] improved usage with new SWT blade forms, referred to by their names coded as SG6040, SG6041, SG6042, and SG6043. In their aerodynamic tests, they saw that SG6040 and SG6041 were capable of higher lifting capability. They found that SG6042 and SG6043 had better lift and drag performance than the other blades, with lower Reynolds numbers. Migliore et al. [22] carried out acoustic tests of 6 blade forms, including the form of FX63-137, and found that the blade forms were suitable for MWTs. Studies on blade forms attempt to achieve new structures with lower Reynolds numbers, less weight, higher lift force, and better capture of kinetic energy of wind.

Two types of axes are important in MWTs: VAWTs and HAWTs. The cut-in of a VAWT is lower than that of a HAWT. However, the efficiency of a VAWT is lower than that of a HAWT [23]. The blades of a HAWT are perpendicular, and the rotation axis is parallel to the direction of wind. There are upwind and downwind types of them. MWTs could be manufactured with gear mechanism and direct drives. Recently, a large number of them have been manufactured with direct drive [5]. The power obtained from a MWT at a certain wind speed is called “nominal power” and the wind speed is called the “nominal wind speed”. According to the British Wind Energy Association (BWEA) and American Wind Energy Association (AWEA) Small Wind Turbine Performance and Safety Standards ([http://smallwindcertification.org/wp-content/uploads/2013/02/bwea\\_small\\_wind\\_performance\\_and\\_safety\\_standard.pdf](http://smallwindcertification.org/wp-content/uploads/2013/02/bwea_small_wind_performance_and_safety_standard.pdf), [http://www.smallwindcertification.org/wp-content/uploads/2011/05/AWEA\\_2009-Small\\_Turbine\\_Standard1.pdf](http://www.smallwindcertification.org/wp-content/uploads/2011/05/AWEA_2009-Small_Turbine_Standard1.pdf)), the nominal wind speed is 11 m/s and the cut-out wind speed should be 20 m/s.

Power performance analyses of manufactured MWTs can be carried out by truck [24], field [25], and tunnel [26] tests. Though the truck and the tunnel tests can be performed in a short time, the field test takes 1–2 years. In order to perform the field test, a large area that has a high wind speed is needed [25]. Such area is not necessary for the truck and the tunnel tests. For the field testing of MWTs, countries that intensively utilize wind energy to generate electricity have founded their own private and national centers [23,25,27]. The truck and the tunnel tests can be carried out by manufacturing firms [25]. Some studies in terms of these tests are performed there. Ozgener [4] set up a SWT at the Solar Energy Institute of Ege University (38.24° N, 27.50° E), in İzmir, Turkey, and he realized the field testing of the SWT. He employed the NACA 63-622 blade form of 3 m in diameter. At a wind speed of 7.5 m/s, he obtained power of 616 W from the SWT. Ani et al. [23] compared 6 commercially available SWTs with regards to energy efficiency and generated electric power at low wind speeds at the Technopark Schoondijke (the Netherlands). They reached the conclusion that SWTs with blade diameter of over 3 m have higher AEPs. Elizondo et al. [24] executed power performance analyses of their own designed MWT giving power of 1.4 kW at 10.5 m/s wind speed by using truck and the field tests. They showed that their MWT could generate power of 2 kWh/day for an average wind speed as low as 3.5 m/s and an air density of 85% of the standard pressure and temperature value in the configuration of 48 V. Whale et al. [25] executed power performance analyses of the SOMA1000 MWT by field test. As a result of their tests, they reached higher efficiency than that given by the SOMA1000 manufacturer. Sahin et al. [26] carried out tunnel tests of their MWT of 100 W and 12 V DC. They found that the MWT had powers of 80 W at a wind speed of 14 m/s and a cut-in wind speed of 2.5 m/s. According to the IEC 61400 standard, Bowen et al. [27] tested the power performance, durability, acoustic, and safety of 5 MWTs having different structures at the National Renewable Energy Laboratory (Golden, CO, USA) and announced their manufacturing firms. Ata et al. [28] set up a commercially available off-grid MWT system giving 3 kWh at the Vocational School Campus of Celal Bayar University in Kırkağaç, Turkey. For the site, they estimated the AEP.

In this study, design, implementation, and power performance analyses of a MWT system, which works off grid and with direct drive and has a PMSG of 10–35 V AC output voltage and 3 blades, feeding a battery group of 12 V DC, are presented. The MWT was configured the HAWT structure. The power performance testing was conducted by truck test. A novel blade form offering better performance at low wind speeds, which enhanced the bearing power and blade strength and reduced friction, formed by modifying the FX63-137 having the blade tip geometry used in augmented-type turbines, was utilized on the MWT blades. A supervisory control and data acquisition (SCADA) system based on a programmable logic controller (PLC) was used to measure and analyze the values of current, voltage, power, and temperature of the MWT in the truck test. The performance coefficient of the MWT was 0.277 at a tip-speed ratio (TSR) of 5.41.

## 2. Materials and methods

### 2.1. Equations for Power Performance Analysis of MWTs

Wind, which provides the energy of a MWT and continuously moves and rapidly changes in the atmosphere, has a certain mass and a kinetic energy. The instantaneous wind power of the MWT is expressed in the following equation [29]:

$$P_w = \frac{1}{2} \cdot \rho \cdot A \cdot v^3, \quad (1)$$

where  $P_w$  is the instantaneous wind power (W),  $\rho$  is the air density ( $\text{kg/m}^3$ ),  $A$  is the cross-sectional area perpendicular to a wind stream ( $\text{m}^2$ ), and  $v$  is wind speed (m/s).

All of the instantaneous wind power is not converted into electrical energy in the MWT. The amount of power converted into electrical energy in the MWT is given by [26]:

$$P_t = \frac{1}{2} \cdot C_p \cdot \rho \cdot A \cdot v^3, \quad (2)$$

where  $P_t$ ,  $C_p$ ,  $A$  ( $A = \pi \cdot R^2$ ), and  $R$  are the generated power of the MWT (W), the power coefficient, the swept area during the rotation of the rotor blades ( $\text{m}^2$ ), and the maximum rotor radius (m) of the MWT, respectively.

The value of the power coefficient is a function of the linear speed ( $u$ ) of the turbine blades at the end point and the wind speed ( $v$ )  $C_p = f(u/v)$ . The  $u/v$  ratio is called the TSR and is symbolized by  $\lambda$ . If the maximum value of electrical power obtained from the MWT is desired, the rotor rotational speed must be arranged according to the wind speed, and the ratio should be continuously kept at the optimum value of  $\lambda = \lambda_{opt}$ . In this case, the power coefficient of the MWT reaches the maximum value. The TSR is defined by [6,24,30]:

$$\lambda = u/v = \omega_t R/v = 2\pi n(rpm)R/60v, \quad (3)$$

where  $\omega_t$  is the mechanical angular speed of the MWT blades (rad/s).  $\omega_t R$  is the linear speed of the MWT blade tip (m/s). The mechanical angular speed depends on frequency  $f$  (Hz, 1/s), and it is defined by  $f = \omega_t/2\pi$ . The mechanical angular speed can be expressed by  $\omega_t = 2\pi n/60$  as a function of the rotational speed of the MWT [31], where  $n$  is the rotational speed of the MWT (rev/min) and it is  $n = 60f$  (rev/s). Depending on the number of poles of the PMSG, the rotation is given by  $n = 60f/2P$ , where  $2P$  is the number of pole pairs of the PMSG.

The power coefficient of a MWT is varied by wind speed. For this reason, the efficiency of a MWT is expressed best by  $C_p-\lambda$  curves. If the electrical equipment and mechanical equipment losses are omitted, the power coefficient of the MWT is given as follows [4,17]:

$$C_p = \frac{P_t}{P_w} = \frac{I \cdot V}{\frac{1}{2} \rho \cdot A \cdot v^3}, \quad (4)$$

where  $I$  and  $V$  are the current (A) and voltage (V) obtained from the MWT, respectively.

As long as the air density is constant in the MWT's environment, the air stream has kinetic energy depending on the wind speed. The kinetic energy of the air stream equals 0 when wind speed equals 0. If there is a constant wind speed, the kinetic energy is given by:

$$E_{kin} = \frac{v^2}{2}, \quad (5)$$

where  $E_{kin}$  is the kinetic energy of wind (J).

To determine the wind power under the influence of the MWT, the mass flow amount of air passing through the MWT rotor per unit time must be known. The mass flow amount of the air  $\dot{m}$  (kg/s) is defined by:

$$\dot{m} = \rho \cdot A \cdot v = \rho \cdot \pi \cdot R^2 \cdot v, \quad (6)$$

where  $A_v$  is the volumetric flow rate of air ( $\text{m}^3/\text{s}$ ).  $\rho$  is an air density ( $\text{kg}/\text{m}^3$ ). The maximum instantaneous power obtained from the wind is then defined as follows:

$$P_w = \dot{m} \cdot E_{kin} \quad (7)$$

Today, many MWTs have efficiency between 20% and 40%, and they convert kinetic energy from the wind into electrical energy. Kinetic energy is a form of mechanical energy and is completely converted into work. Hence, the exergy of kinetic energy or the work potential of a system equals its own kinetic energy regardless of its temperature and pressure. Another variable affecting the input power in a MWT is the site air density. According to International Standard Atmosphere conditions, the air density equals  $1.225 \text{ kg}/\text{m}^3$  at sea level,  $15^\circ \text{C}$  temperature, and  $1013.25 \text{ mbar}$  ( $1 \text{ mbar} = 98 \text{ Pa}$ ,  $1 \text{ atm} = 101,300 \text{ Pa}$ ) atmosphere pressure. The air density and the atmosphere pressure reduce when rising from sea level. Thus, the generated power of the MWT also decreases. The air density per unit volume is expressed by the following equation:

$$\rho = \frac{P}{287 \cdot T}, \quad (8)$$

where  $P$  is the atmosphere pressure of air (Pa),  $287$  is the constant gas coefficient of air ( $\text{J}/\text{kg K}$ ), and  $T$  is the ambient temperature in Kelvin ( $^\circ \text{C} + 273.12 = \text{K}$ ).

Different software can be used for the calculation of the AEP of MWTs. It is known that the power curve of the MWT and the annual wind speed probability distribution of the installation site are needed to calculate the AEP. The power curve of the MWT is determined by analysis. To determine the annual wind speed probability distribution, 2 probability distribution functions, Rayleigh and Weibull, are used. The Weibull probability distribution function is given by [32]:

$$hw(v) = \frac{k}{C} \cdot \left(\frac{v}{C}\right)^{k-1} \cdot \exp\left[-\left(\frac{v}{C}\right)^k\right], \quad (9)$$

where  $hw(v)$ ,  $k$ , and  $C$  are the Weibull probability distribution function, the parameter showing wind speed distribution or shape parameter, and the relative cumulative frequency or scale parameter, respectively. In the Weibull probability distribution function, there are 2 unknown parameters,  $k$  and  $C$ . Analytical and empirical equations are used to find them.

The Rayleigh probability distribution function is defined by the following equation [32]:

$$h_R(v) = \frac{\pi}{2} \cdot \frac{v}{v_m^2} \cdot \exp\left[-\left(\frac{\pi}{4}\right) \cdot \left(\frac{v}{v_m}\right)^2\right], \quad (10)$$

where  $h_R(v)$  is the Rayleigh probability distribution function and  $v_m$  is the average wind speed (m/s). In the Rayleigh probability distribution function, there is one unknown parameter,  $v_m$ .

In the end, the AEP of the MWT is given by [23]:

$$E = t \int_{v_{min}}^{v_{max}} P_t(v) \cdot f(v) \cdot dv, \quad (11)$$

where  $E$  is the AEP ( $\text{kWh}/\text{year}$ ),  $v_{min}$  is the cut-in wind speed,  $v_{max}$  is the cut-out wind speed,  $f(v)$  is the wind speed distribution function, and  $t$  is the annual time in hours ( $1 \text{ year} = 8760 \text{ h}$ ).

## 2.2. The truck test and the installed measurement system

The truck test was selected to carry out the power performance analyses of the designed and implemented MWT, because it is a faster and cheaper test than the field and tunnel tests. A 2010 model Volkswagen/Transporter model with a double cabin was utilized as the trucker. The setup of the MWT on the trucker is shown in Figure 1a.



**Figure 1.** (a) The truck test; (b) the setup of the measuring system of the MWT.

In Figure 1a, the MWT has been mounted to the top of a tower-framed iron pipe 3.5 m in length and 48.2 mm in diameter. The tower has been fixed on the ground of the trucker on the right, left, and front sides by tie wires. In addition, the feet of the tower have sandbags on them, and the risk of the tower tipping is thus minimized at higher trucker speeds. For the measurement of wind speeds, 2 different vane-type anemometers were used for calibrations in the wind tunnel; the first was a Prova AVM-03 model having  $\pm 3\%$  accuracy at 0.3–45 m/s wind speed, while the other was a Kestrel 3000 model having  $\pm 3\%$  accuracy at 0.6–40 m/s wind speed. One of them was placed at the bottom of the tower, not affected by the wind of the MWT. The other was located to the top left of the trucker to measure the wind speed. A digital multimeter was utilized as a frequency meter, a BM805 model having  $\pm 0.5\%$  accuracy, to find out the generated power in reference to the frequency. A photo tachometer, an Extect Pocket TACH 461700 model having  $\pm 3\%$  accuracy and capable of measuring 10–20,000 rpm, was also used to measure the rotor speed in rpm. In addition, a differential data receiver, an Extect HD200 model having  $\pm 1\%$  accuracy and capable of measuring  $-300$  to  $1372$  °C, was employed to measure the temperature by altitude of the MWT and the ambient temperature. In order to calculate the value of the air density, air pressure data from the test day were taken from the Turkish State Meteorological Service (Turkish abbreviation: DMI).

A SCADA system based on the PLC was employed to measure and analyze the values of current, voltage, power, and temperature of the MWT in the truck test. The SCADA and the battery group are presented in Figure 1b. In the measurement system in Figure 1b, a current transmitter, which is a WeidMüller WAS2 CMA 40/50/60 A model having  $\pm 1\%$  accuracy and capable of measuring 0–60 A, is utilized to find out the generated current of the MWT. A voltage transmitter, which is a Phoenix Contact MCR-VDC-UI-B-DC model having  $\pm 1\%$  accuracy and capable of measuring 0–550 V DC, was used to measure the generated voltage of the MWT. The outputs of current and voltage transmitters were connected to a Siemens Simatic S7-200 CPU224XP DC/DC/DC model PLC. The obtained data of the PLC could be instantaneously monitored at

the Siemens TD200 operator panel (OP) by the written OP software. Furthermore, the values of 4 different temperatures, from the core of the MWT, the tower's top, the tower bottom's, and the environment, were measured by the EM231 thermocouple expansion module of the PLC. The data were moved and registered to be analyzed by the computer and Fultek-WinTr SCADA software. The electrical connections of the MWT and the electrical measurement system based on a PLC are presented in Figure 2. The PLC-SCADA flow diagram is given in Figure 3. The handled measurement devices were also employed for the measurements of current and voltage, in addition to the SCADA system. A digital ammeter, a Brymen BM805 model having  $\pm 0.5\%$  accuracy and capable of measuring 10 A, was used to find the current value up to 10 A. A digital voltmeter, a being Brymen BM805 model having  $\pm 0.5\%$  accuracy, was continuously employed to measure the voltage value with the SCADA system.

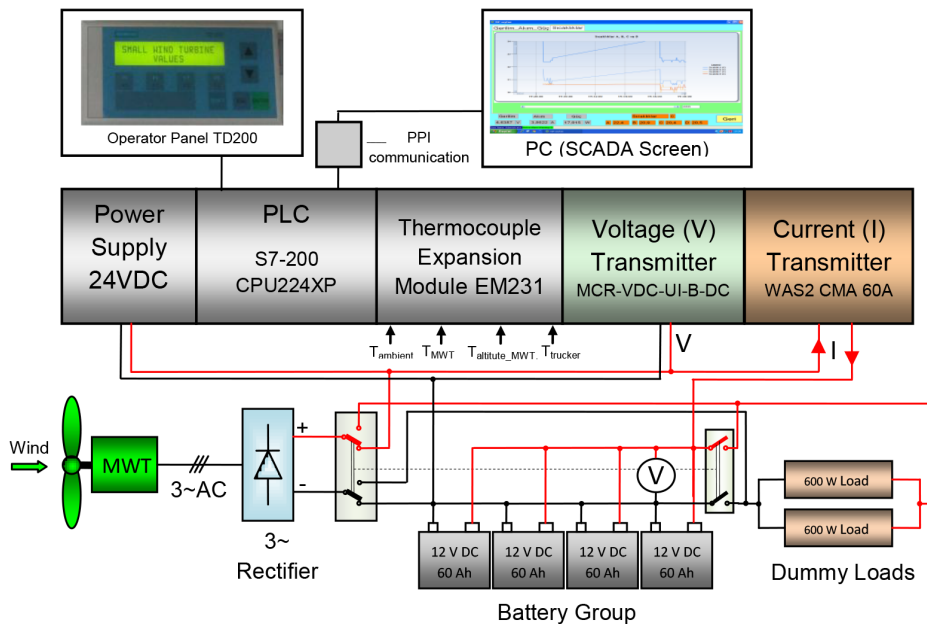


**Figure 2.** The electrical connections of the MWT and the electrical measurement system with a PLC.

Four battery packs of 12 V and 60 A, connected to the each other in parallel, were used to charge the device in the battery group. The 3-phase AC voltage was converted to DC voltage by the 3-phase bridge rectifier and the DC voltage was then connected to the battery group. First, the battery group was discharged down to 10.5 V via 2 loads of 600 W. When the battery group charged to 13.5 V, it was again discharged to 10.5 V via 2 loads of 600 W. Due to the fact that the value of current obtained from the MWT was high, NYAF wire having capacity of 80 A of 10 mm<sup>2</sup> in the open air was used for cabling.

### 3. Design and implementation of the MWT

The designed and implemented parts of the MWT consist of a body, a PMSG, 3 blades and a tie, a tower, and electrical equipment. The original PMSG and a general view of the MWT are given in Figure 4.

#### 3.1. The Body of the MWT

The body of the MWT was made of solid cast aluminum. In order to naturally dissipate the heat of the stator of the MWT, the aluminum material in the body was used. The heat losses generated due to the high current

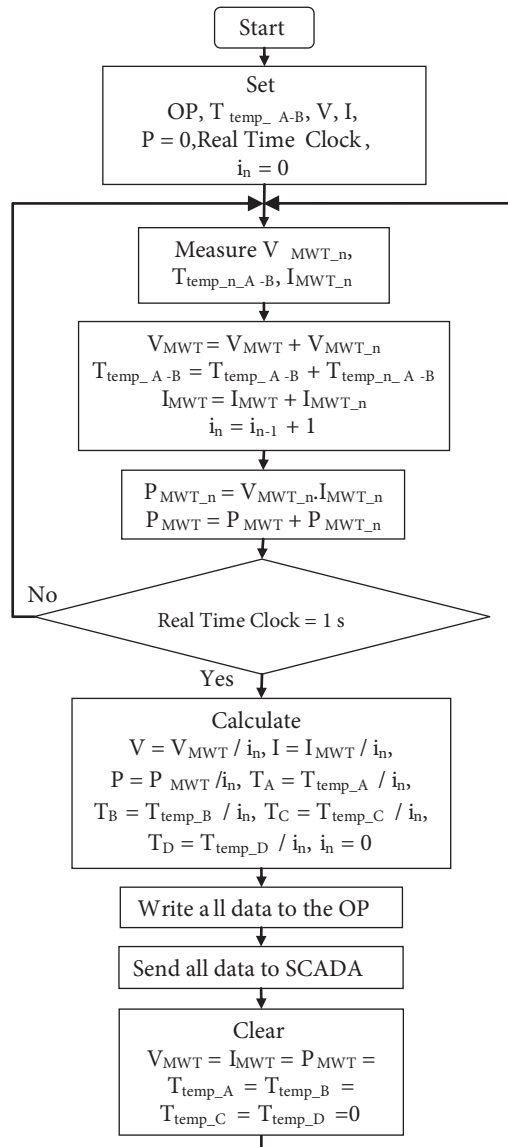


Figure 3. The PLC-SCADA flow diagram.

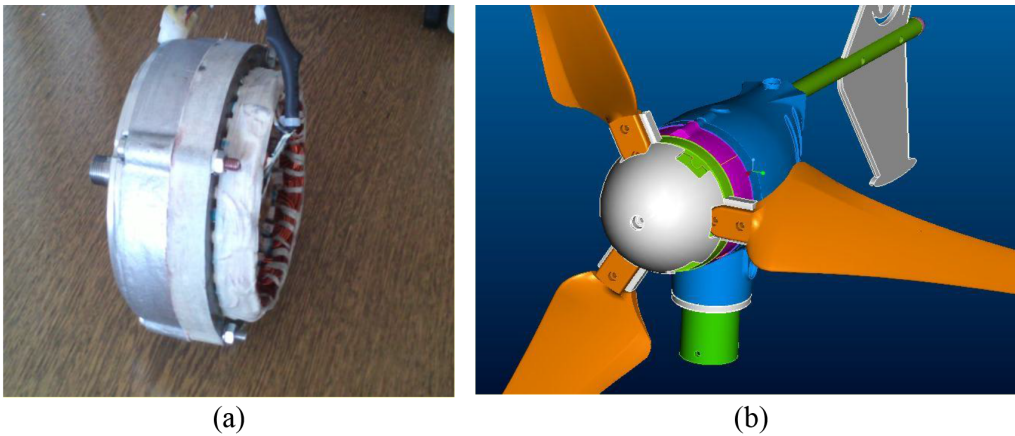


Figure 4. (a) The original PMSG; (b) the general view of the MWT.



in the stator were thus minimized. A hole, 5 mm in diameter, was made to the tie subregion of the body to observe the temperature of the stator during operation. The temperature of the stator was measured by a T-type point-ended thermocouple connected to the EM231 module and inserted into the hole. The temperature was increased to a maximum of 70 °C at the stator current of 40 A.

### 3.2. The PMSG of the MWT

An original direct-drive PMSG that reduced the cogging torque via the fractional winding technique optimization of the number of grooves and the poles ( $Q_s/2p$ ) was used. The original PMSG was designed and manufactured as 12 pairs of poles. The output voltage of it was 3-phase 12 V AC. The output voltage was varied from 10 V AC to 35 V AC at 2.7–20 m/s wind speeds. The PMSG shaft was made of stainless steel so as to not affect the magnetic field. The magnet form that was angularly balanced and asymmetrically placed was employed in order to reduce the cogging torque at the lower wind speeds in the PMSG. At the same time, the surfaces facing the stator sheets of the PMSG magnets were shaped in herringbone form for minimum cogging torque [8–14]. The cross-sectional view of the rotor, the stator, and the bedding of the PMSG is given in Figure 5. The dimensions of the PMSG with rotor and stator are given in Table 1.

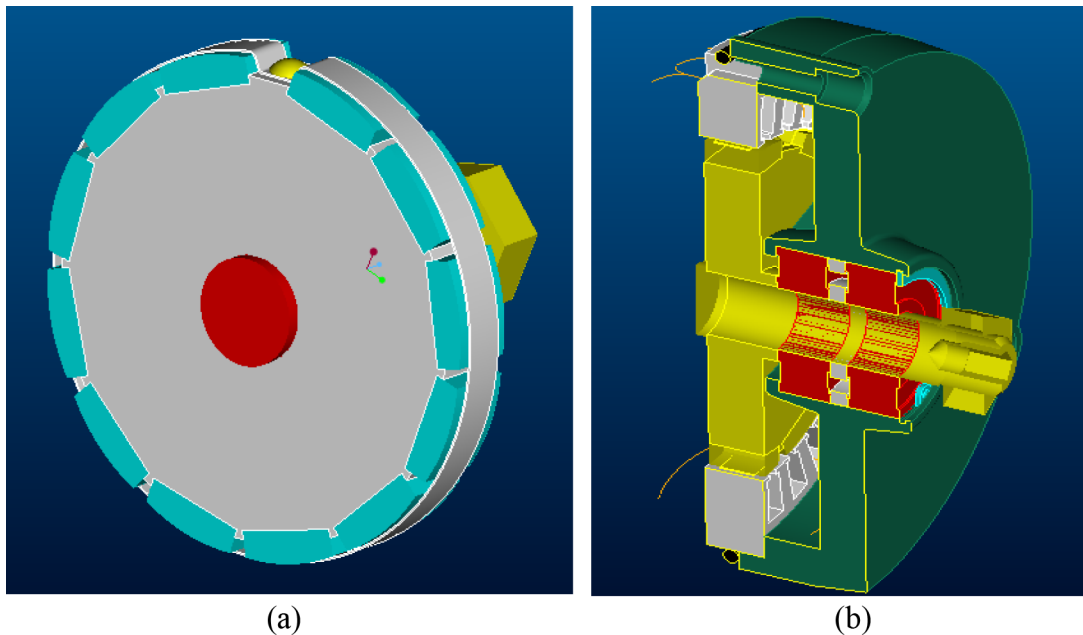


**Figure 5.** The cross-sectional view of (a) the rotor and (b) the stator and the bedding.

**Table 1.** The dimensions of the PMSG with stator and rotor.

Features	Value	Features	Value
Number of stator slots	36	Slot height	11 mm
External diameter of the stator stack	150 mm	Number of poles	12
Internal diameter of the stator stack	99 mm	Thickness of magnet	6 mm
Length of the stator stack	20 mm	Rotor material	1040 steel
Slot width	7 mm	Length of air gap	1 mm
Slot opening width	3 mm	Silicon-laminate sheet thickness	0.50 mm
Rotor shaft diameter	20 mm	Inner diameter of the rotor bearing	20 mm
Rotor shaft length	110 mm	Outer diameter of the rotor bearing	40 mm

The generated 3-phase AC was transmitted from the slip rings to the bottom of the tower by the electrical cables. Thus, the electrical equipment at the top of the tower was less. Otherwise, if any fault in the electrical equipment occurred at the top of the tower, the tower could fall or a person would have to climb to the tower to repair the fault. Hence, maintainability was provided.

### 3.3. The blades and the tail of the MWT

A novel blade form offering better performance at low wind speeds was utilized for the MWT blades, which enhanced the bearing power and blade strength and reduced friction, formed by modifying the FX63-137 and SG6043 with the blade tip geometry used in augmented-type turbines. In order to increase the lifting capacity, the blades were twisted at an angle of  $30^\circ$  from 70% of blade length, being the starting from the trailing edge reference point. A blade form with higher lifting capacity than the normal blade form was thus obtained. The blade form and the angle of repose were designed considering the distance from the center of the blade and the calculated Reynolds number. The usage of the blade form having the best coefficient in Reynolds numbers was ensured. So as to increase the lifting capacity, the gurney flaps commonly used on race cars were also employed as parts of the trailing edge. Thus, during plastic injection, both the flow of the liquid material was facilitated and the blade lifting capacity was increased. On the other hand, the gurney flaps were used until 80% of the blade length so that the rotation of the blades at high wind speeds would not affect them. In addition, the form of a horse mane made up of micro scratches was implemented to reduce friction to the back part of the blade. Thus, it was observed that both the blades had high lifting capacity and a blade form could reach high rotational speeds. Figure 6 shows the blade form employed in the MWT.

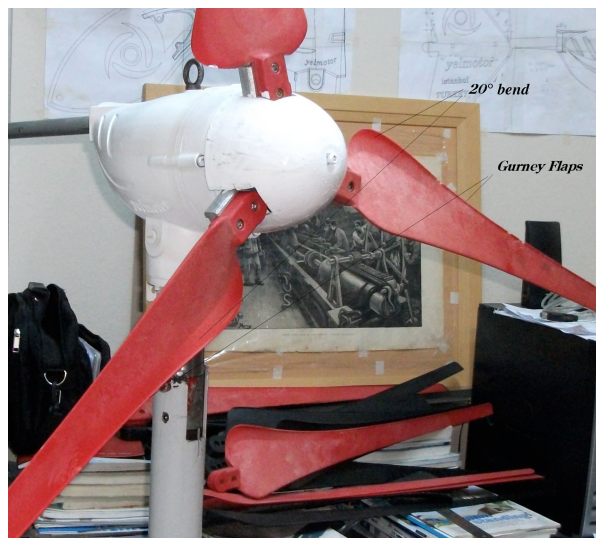


**Figure 6.** The usage blades form on the MWT.

The MWT was designed with 3 and 5 blades. The power performance analyses were carried out with 3 blades. The 5-bladed version of the MWT was also developed to use in regions having low average wind speeds.

The tail structure of the MWT was designed in a modular form. It was mounted to the body by an iron pipe of 2.54 cm to provide more rapid response to the wind change. The tail was made of PVC material.

### 3.4. The tower of the MWT

The heights of MWT towers vary by setup sites. According to the IEC 61400 standard, it is suitable that a MWT tower have a height of 10–18 m in outdoors areas, except on the roofs of apartments or workplaces.

### 3.5. Electrical equipment of the MWT

The electrical connections of the MWT were designed and manufactured to be at the bottom of the tower. The 3-phase output of the MWT was converted into DC by the 3-phase rectifier. The output of the rectifier was directly connected to the battery group. Due to the fact that the battery group has large capacity, it behaves as an unlimited current receiver. When the battery group was charged by the MWT in the truck test, it was discharged by 2 loads of 600 W. The voltage of the battery group changed between 10.5 and 13.5 V. For carrying out the power performance test analyses, this system was set up off-grid. If required, it can be changed to on-grid by additional devices and by changing the electrical connection.

The general characteristics of the designed, implemented, and carried out power performance analyses of the MWT are defined in Table 2.

**Table 2.** The general characteristics of the MWT.

Features	Value	Features	Value
Rotor diameter	1.24 m	Braking	Electrical
Rotor-swept area	1.207 m <sup>2</sup>	Generator type	PMSG
Number of blades	3	Number of poles	12
Nominal power	177 W	Output phase (1/3)	3-phase
Output voltage	10–35 V AC	Annual energy production	384 kWh
Body structure	Aluminum	Upwind-downwind	Upwind
Weight	12 kg	Direction of rotation	Clockwise
Axis type VAWT-HAWT	HAWT	Off/on-grid	Off-grid
Wind direction adjustment mechanism (YAW)	Tail	Highest design wind speed	25 m/s
Cut-in wind speed	2.7 m/s	Highest temperature of the stator	90 °C
Nominal wind speed	11 m/s	Design life	20 years
Cut-out wind speed	20 m/s	Maximum power (20 m/s)	524 W

## 4. Results and discussion

MWTs have different power curves depending on their structures and types. Power curve and other analyses of the manufactured MWT were done with the resulting data obtained from the truck test. The truck test was done in a flat area at 40° 36'N, 33° 37'E in Çankırı, Turkey. The ambient temperature and the air pressure on the test day were taken from the DMI. According to DMI data, the temperature and the pressure were 27.9 °C (27.9 °C + 273.12 = 301.02 K) and 1015.1 hPa, respectively. Output data of the MWT were taken at up to a maximum of 20 m/s wind speed in the truck test. Tests at over 20 m/s wind speed were only done observationally. At about 25 m/s wind speed, bending occurred to the blades of the MWT. Therefore, the maximum wind speed should be taken as 20 m/s for the circuit design of the electronic braking to the MWT. In LWTs, the rotation speed control is implemented by pitch control.

The MWT commenced the electricity generation at 2.7 m/s wind speed, the cut-in wind speed. The air density observed on the test day was calculated as  $\rho = 1.152 \text{ kg/m}^3$  from Eq. (8) with the meteorological data of the DMI. The radius and the area of the MWT blades were  $R = 0.62 \text{ m}$  and  $A = 1.207 \text{ m}^2$ ,

respectively. After these calculations, the kinetic energy  $E_{kin}$ , the mass flow amount of air  $\dot{m}$ , and the maximum instantaneous wind power  $P_w$  of the MWT were calculated from Eqs. (5), (6), and (7), respectively. Moreover, the instantaneous wind power to the MWT was calculated from Eq. (1) depending on the rotor-swept area. Figures 7 and 8 show the calculated results of all data of the MWT.

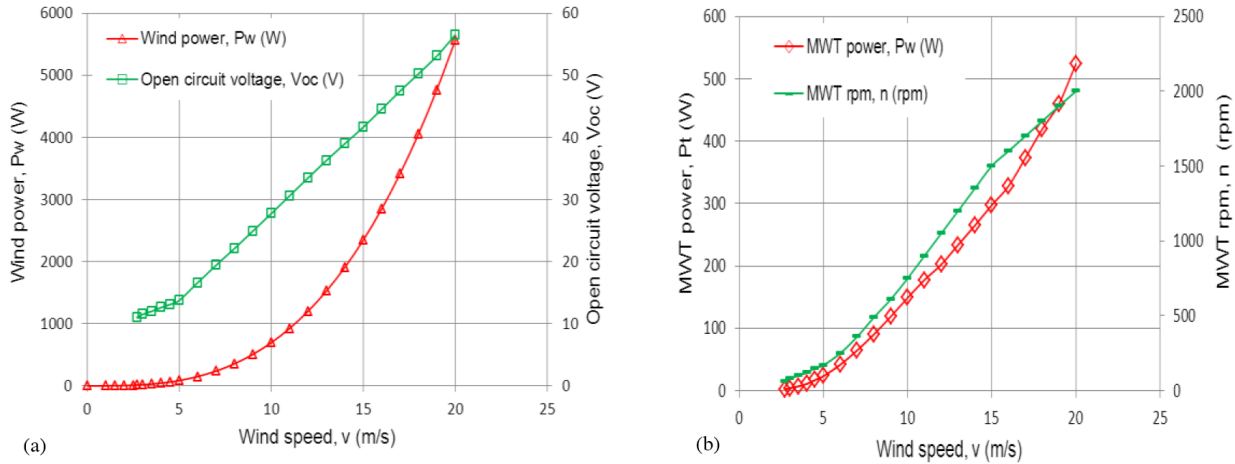


**Figure 7.** (a) The open circuit voltage  $V_{OC}$  and the instantaneous wind power  $P_w$ , and (b) the generated power  $P_t$  and the rotation  $n$  of the MWT for different wind speeds  $v$ .

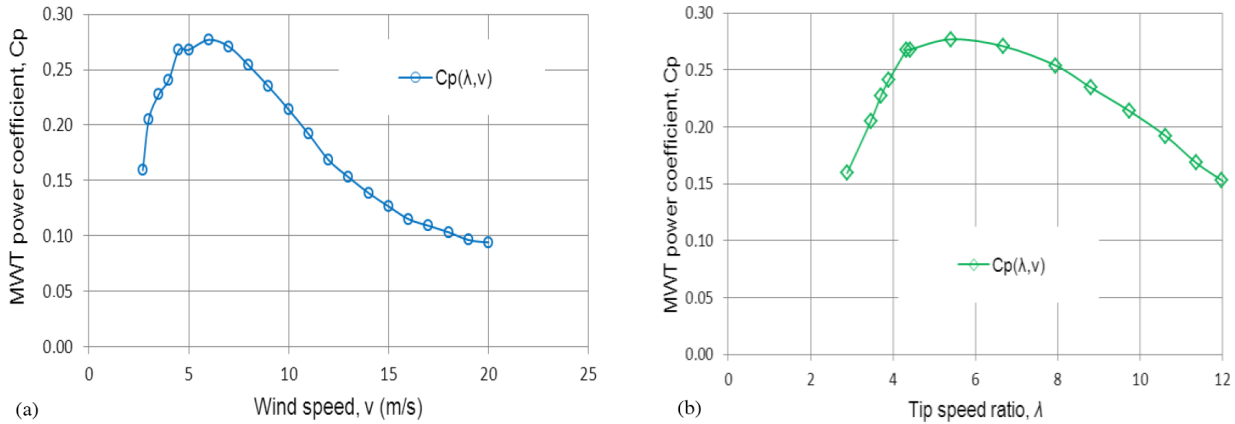


**Figure 8.** (a) The power coefficient  $C_p$  curve depending on wind speed, and (b) the power coefficient  $C_p$  curve depending on the TSR of the MWT.

The instantaneous wind power,  $P_w$ , of the MWT increases in cubic relation to the wind speed. When there is no load to the end of the MWT, the MWT rotates at free speeds. Depending on the increase of the wind speed, the rotation  $n$  and the open circuit voltage  $V_{OC}$  of the MWT increase linearly. The PMSG was constructed of 12 pairs of poles and hence the revolutions per minute  $n$  were determined depending on frequency from  $n = 60f/2P$  (rpm).

Depending on the wind speed under the influence of the MWT, the open circuit voltage  $V_{OC}$  measured from across the output of the 3-phase rectifier and the instantaneous wind power  $P_w$  of the MWT are given in Figure 7a. Furthermore, depending on the wind speed, the rotational speed  $n$  and the generated power  $P_t$  of the MWT are given in Figure 7b. Considering data in Figure 7a, for some wind speeds  $v$ , the open circuit

voltage  $V_{OC}$ , the rotation  $n$ , and the instantaneous wind power  $P_w$  of the MWT were, at  $v = 5$  m/s,  $P_w = 86.87$  W,  $V_{OC} = 13.8$  V, and  $n = 170$  rpm; at  $v = 10$  m/s,  $P_w = 694.99$  W,  $V_{OC} = 27.7$  V, and  $n = 750$  rpm; at  $v = 15$  m/s,  $P_w = 2345.59$  W,  $V_{OC} = 41.6$  V, and  $n = 1500$  rpm; and, at  $v = 20$  m/s,  $P_w = 5559.91$  W,  $V_{OC} = 56.5$  V, and  $n = 2000$  rpm, respectively.

In the MWT tests, the generated 3-phase AC electricity was converted into DC by a 3-phase bridge rectifier, and then the output of the rectifier was connected to the battery group having 4 batteries of 60 A and 12 V connected in parallel. The current and the voltage of the battery group, generated by the MWT, were measured by a voltmeter, an ammeter, and a SCADA system. The instantaneous voltage, the current, and 4 temperatures were monitored by the OP and recorded to the computer by the SCADA program. First, the battery group was discharged down to 10.5 V via 2 loads of 600 W. During the truck test, when the battery group was charged to 13.5 V by the MWT, it was again discharged down to 10.5 V. This event continued throughout the truck test. Hence, the battery group was an unlimited current receiver. The current of the MWT was monitored by both a digital ammeter and the SCADA until 10 A. After 10 A, the current of the MWT was only monitored and registered by the SCADA program.

By means of a new SCADA program based on a PLC, given in Figure 2 describing the electrical connections of the MWT, and the electrical measurement system with a PLC given in Figure 3 describing the PLC-SCADA flow diagram, the current, the voltage, and 4 different temperature values of the MWT were measured and registered. This is the first time SCADA based on a PLC has been used in truck testing. At the same time, the monitoring of instantaneous data was carried out by the OP. The registering was performed every 1 s in the SCADA program. In the PLC, the average values every 1 s was taken instead of the instantaneous values of the current, the voltage, and temperatures. The real-time clock of the PLC was utilized for the average values every 1 s. The average power value at a certain wind speed every 1 s was also calculated and transferred to the SCADA program along with other data. During the truck test, the measurements of wind speed, rotor rotational speed, and rotor frequency were accomplished by handheld devices. If a wind transmitter and a frequency transmitter had been used and the values from them had been transferred to the SCADA based on the PLC, the measurements and registering would have been more comfortable. Nevertheless, the transferring of certain values to the SCADA provided great convenience. The use of a current transmitter in taking high current values is a factor of convenience.

Depending on wind speed  $v$ , the curve of the calculated power  $P_t$  of the MWT from the measuring data of current  $I$  and voltage  $V$  is given in Figure 7b. When Figure 7b is analyzed, the beginning of the conduction of power to the battery group from the MWT was at 2.7 m/s wind speed. In this case, current  $I$ , voltage  $V$ , and power  $P_t$  of the MWT were 0.2 A, 10.5 V and 13.68 W, respectively. For 10, 15, and 20 m/s wind speeds, current  $I$ , voltage  $V$ , and power  $P_t$  of the MWT were  $I = 11.6$  A,  $V = 12.8$  V, and  $P_t = 148.71$  W;  $I = 22.6$  A,  $V = 13.2$  V, and  $P_t = 297.19$  W, and  $I = 38.5$  A,  $V = 13.6$  V, and  $P_t = 523.60$  W, respectively.

When the values of current and voltage obtained from the MWT are analyzed, it is seen that there was no restrictive effect on the rotational speed of the MWT owing to the unlimited current capacity of the battery group. The voltage of it reached a maximum of 13.5 V. The overwhelming increase in power of the MWT was fulfilled via the increase in current. It was noticed that while the current value increased from 1.9 A to 38.5 A, the increase in voltage value was from 10.5 to 13.6 V. According to AWEA standards, the reference power of the MWT was achieved at 177.47 W at the reference wind speed of 11 m/s.

In Figure 8a, the power coefficient  $C_p$  curve of the MWT is given depending on the truck test data. The power coefficient  $C_p$  curve was calculated from 2.7 m/s wind speed, by reason of the fact that the MWT began to generate electricity at the cut-in wind speed of 2.7 m/s. When analyzing Figure 8a where the wind speed

has become equal to about 6 m/s, the highest power coefficient was achieved as  $C_p = 0.277$ . For wind speed values of 5, 10, 15, and 20 m/s, the power coefficient value  $C_p$  of the MWT was  $C_p = 0.268$ ,  $C_p = 0.214$ ,  $C_p = 0.127$ , and  $C_p = 0.094$ , respectively. While the wind speed was between 5 and 10 m/s, the power coefficient  $C_p$  of the MWT demonstrated a better performance between 0.277 and 0.214 with respect to the other wind speed values.

The TSR is a common and useful value for the scaling of parameters of a WT. In addition, it is important to combine the aerodynamic effects of wind speed such as rotor size, power coefficient, and angular speed for a WT. The power coefficient define the response of a WT under different operating conditions. In Figure 8b, the power coefficient of the MWT is given depending on the TSR. Initially, as the TSR increased, the power coefficient increased. After the power coefficient reached the maximum value at the specific value of the TSR, it began to decrease. This is explained as follows: for the small values of the TSR, almost all of the wind passes across the blades without the majority of power transfer to the WT due to the slow rotation of the blades, and, for the large values of the TSR, the blades act as a solid disk due to the rapid rotation of the blades; as a result, the power coefficient decreases. Ultimately, the TSR directly affects the generated power of the MWT. Taking into account the best TSR is very critical for design of a turbine blade. While the TSR values of LWTs normally are between 7 and 10, this value is between 2 and 4 for many small-scale wind energy portable turbines [33]. Prior studies have shown that this value is between 3 and 7 for MWTs and SWTs [17,24,28]. In this study, the maximum power coefficient was  $C_p = 0.277$  for  $TSR = 5.41$  as shown in Figure 8b.

For the AEP of the MWT, the Rayleigh wind speed distribution in Eq. (10) was used. According to AWEA standards, where the calculated total energy would be produced during a 1-year period at an average wind speed of 5 m/s, assuming a Rayleigh wind speed distribution and 100% availability, the average wind speed was taken as 5 m/s and the Rayleigh wind speed distribution in Eq. (10) was established. In Eq. (11),  $v_{min} = 2.7$  m/s was the cut-in wind speed,  $v_{max} = 20$  m/s was the cut-out wind speed, and  $t = 8760$  h was the value of annual hours. As a result, the AEP obtained from the MWT was calculated as 384 kWh/year.

Large-diameter MWTs usually have lower electricity costs than small-diameter MWTs. On the other hand, many small-diameter MWTs exhibit higher AEP efficiency per rotor-swept area than large-diameter MWTs. A comparison between the designed system and commercial systems is given in Figure 9. In making this comparison, the comparisons of a study done by Ani et al. [23] were taken into account. In their study, the AEPs and the performance coefficients given by the manufacturers were found comparable to their experimental measurements. Taking into this account, 5 MWTs were compared to each other in our study. Four of the MWTs were the MWTs tested by Ani et al. [23]. The remaining MWT is ours. The branding and power of the compared MWTs are the Fortis Passaat at 1.4 kW, Swift at 1.5 kW, Zephyr Air Dolphin at 1 kW, Ampair at 0.6 kW, and our MWT.

On account of the fact that the 5 rotor diameters and the powers of the compared MWTs differ, 2 criteria have been used for a fair comparison. The first of these is the AEP per swept area (kWh/m<sup>2</sup>), and the second is the cost of generated electricity (€/kWh). The AEP and the performance coefficient of MWTs are incorrectly estimated by many manufacturers. Therefore, the MWTs could not provide the AEP given by the manufacturers at the installed sites and could not produce the predicted performance. This study is of great importance in view of defining the power performance curve and the amount of AEP of the designed and implemented MWT. The device optimization was carried out by reference to these data. Studies of the optimized blade model, the body aerodynamics, and the optimized PMSG were fulfilled with the data.

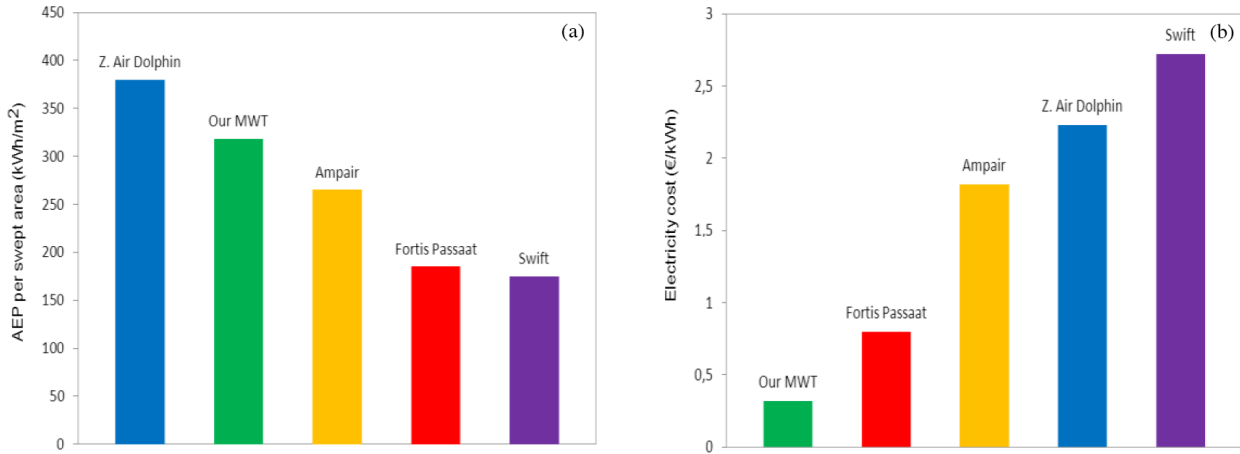


**Figure 9.** The comparison between the designed MWT system and commercial MWT systems with respect to (a) AEP per rotor-swept area and (b) electricity costs.

The AEP values of the compared MWTs were taken at 5 m/s wind speed. In this situation, the AEP value per swept area of the Fortis Passaat of 1.4 kW, of Swift of 1.5 kW, of Zephyr Air Dolphin of 1 kW, and of Ampair of 0.6 kW from Figure 9 and [23] is 185 kWh/m<sup>2</sup>, 175 kWh/m<sup>2</sup>, 380 kWh/m<sup>2</sup>, and 265 kWh/m<sup>2</sup>, respectively. The AEP value of our MWT is 384 kWh/year. The rotor-swept area is 1.207 m<sup>2</sup>. According to the values, the AEP per swept area of our MWT is about 318 kWh/m<sup>2</sup>. The obtained values are given in Figure 9a. When attention is paid to Figure 9a, the AEP value per swept area of our MWT with a modified new blade model and PMSG that reduced cogging torque is found to be at acceptable levels.

A comparison with regard to the cost of generated electricity (€/kWh), being the second comparison criterion, is given in Figure 9b. The cost of generated electricity was found using the following equation [23]:

$$c = \frac{C_e}{T \times E}, \quad (12)$$

where  $c$ ,  $C_e$ ,  $T$ , and  $E$  are the cost of the generated electricity (€/kWh), the actual system cost (€), the lifespan of a MWT (years), and the AEP (kWh/year) of a MWT, respectively. The costs of the generated electricity of the Fortis Passaat of 1.4 kW, Swift of 1.5 kW, Zephyr Air Dolphin of 1 kW, and Ampair of 0.6 kW from [23] are found to be 0.8 kWh/m<sup>2</sup>, 2.72 kWh/m<sup>2</sup>, 2.23 kWh/m<sup>2</sup>, and 1.82 kWh/m<sup>2</sup>, respectively. The actual system setup cost of our MWT is 2500 €. The cost of the generated electricity was calculated as 0.32 €/kWh. The lifespan of our MWT was taken as 20 years for uniformity with [23]. It was assumed that the MWT would operate during its lifespan. Additional costs such as repairs and maintenance were neglected. It should be noted here, however, that the lifespan of each MWT depends on the process of design and production. The compared data are given in Figure 9b. The cost value of the generated electricity of our MWT is the best value among the compared MWTs in Figure 9b. The cost analysis of the generated electricity is a good criterion for the cost analysis of our MWT. A summary of the performance results of the MWT study is given in Table 3.

While the AEP per swept area (kWh/m<sup>2</sup>) shows the energy conversion efficiency of a MWT, the cost of the generated electricity (€/kWh) represents the cost-effectiveness of a MWT. However, the AEP per swept area energy efficiency (kWh/m<sup>2</sup>) is less important than the cost of generated electricity (€/kWh) in terms of overall performance of a MWT. The energy efficiency of a MWT can be enhanced by the increase of the



**Table 3.** Summary of the performance results of the MWT (AEP per swept area = 318 kWh/m<sup>2</sup>, electricity cost = 0.32 €/kWh).

Measured values (ambient temperature = 27.9 °C, atmosphere pressure = 1015.2 hPa, air density $\rho = 1.152 \text{ kg/m}^3$ )				Calculated values								
Wind speed, $v$ (m/s)	Open circuit voltage, $V_{oc}$ , (V)	Current, $I$ (A)	Voltage, $V$ (V)	Rotor frequency, $f$ (Hz)	Kinetic energy, $E_{kin}$ (W)	Mass flow amount of the air, $\dot{m}$ (kg/s)	MWT input wind power, $P_r$ (W)	MWT output power, $P_t$ (W)	Power coefficient, $C_p$ (-)	Rotor rotational speed, $n$ (rpm)	Mechanical angular speed, $\omega_t$ (rad/s)	Tip speed ratio (TSR), $\lambda$ (-)
2.7	11.0	0.2	10.9	6	4	3.75	13.68	2.18	0.159	60	38	2.88
3	11.5	0.4	11.0	8	5	4.17	18.76	3.85	0.205	80	50	3.46
3.5	12.0	0.6	11.3	10	6	4.86	29.80	6.78	0.228	100	63	3.71
4	12.6	0.9	11.9	12	8	5.56	44.48	10.71	0.241	120	75	3.89
4.5	13.1	1.4	12.1	15	10	6.25	63.33	16.94	0.267	150	94	4.33
5	13.8	1.9	12.3	17	13	6.95	86.87	23.28	0.268	170	107	4.41
6	16.6	3.3	12.6	25	18	8.34	150.12	41.58	0.277	250	157	5.41
7	19.4	5.1	12.7	36	25	9.73	238.38	64.57	0.271	360	226	6.67
8	22.1	7.1	12.7	49	32	11.12	355.83	90.31	0.254	490	308	7.95
9	24.9	9.3	12.8	61	41	12.51	506.65	118.85	0.235	610	383	8.80
10	27.7	11.6	12.8	75	50	13.90	694.99	148.71	0.214	750	471	9.73
11	30.6	13.8	12.9	90	61	15.29	925.03	177.47	0.192	900	565	10.62
12	33.5	15.7	12.9	105	72	16.68	1200.94	202.22	0.168	1050	659	11.36
13	36.3	18.1	12.9	120	85	18.07	1526.89	233.49	0.153	1200	754	11.98
14	39.0	20.2	13.1	135	98	19.46	1907.05	264.62	0.139	1350	848	12.52
15	41.6	22.6	13.2	150	113	20.85	2345.59	297.19	0.127	1500	942	12.98
16	44.5	24.9	13.2	160	125	22.24	2847.67	327.93	0.115	1600	1005	12.98
17	47.5	28.1	13.3	170	145	23.63	3414.48	372.89	0.109	1700	1068	12.98
18	50.2	31.2	13.4	180	162	25.02	4053.17	419.02	0.103	1800	1130	12.98
19	53.1	33.9	13.6	190	181	26.41	4766.93	459.68	0.096	1900	1193	12.98
20	56.5	38.5	13.6	200	200	27.80	5559.91	523.60	0.094	2000	1256	12.98



rotor diameter, being a widely used practice for low wind speeds during its design. In addition, the cost of the generated electricity is an optimization criterion utilized by manufacturers. Hence, in this study, the importance of starting energy generation of MWTs at low wind speeds has been emphasized since MWTs are widely employed where there is no electrical grid. Average wind speeds may be lower in such areas. In this case, a low cut-in is demanded from MWTs. The MWTs having low cut-in values provide higher energy efficiency.

The power performance of LWTs is better than that of MWTs due to the optimized blade forms. The optimization studies of MWTs continue over blade forms, body aerodynamics, and PMSGs to increase the power performance of MWTs.

## 5. Conclusions

In this study, the design, manufacturing, testing, and comparison of an original MWT system constructed with a HAWT axis were presented. The power performance analyses of it were executed by truck test. In the MWT system, an original PMSG reduced cogging torque via the fractional winding technique optimization of the number of grooves and the poles ( $Q_s/2p$ ), with the magnet forms angularly balanced and asymmetrically placed and the herringbone form utilized. Furthermore, a novel blade form offering better performance at low wind speeds was utilized for the MWT blades, enhancing the bearing power and blade strength and reducing friction, formed by modification of the FX63-137 with the blade tip geometry used in augmented-type turbines. The following conclusions were reached from the MWT truck test:

- The MWT began electricity generation at 2.7 m/s cut-in wind speed with the employed new blade form and the PMSG reduced cogging torque.
- The power coefficient of the MWT was achieved as  $C_p = 0.277$  at  $TSR = 5.41$ . In this case, the generated power of the MWT was  $P_t = 41.58$  W.
- In addition, for the measuring, monitoring, and registering of the output electrical values of the MWT, a new SCADA system-based PLC was designed, programmed, and used in the MWT system. Thanks to the SCADA system, the analyses of the output electrical data of the MWT system could be made in greater detail.
- The power performance curve of the MWT was obtained.
- When wind speed was 20 m/s, the generated maximum power of the MWT was 523.60 W. For the MWT, the maximum wind speed should be defined as 20 m/s.
- The AEP that would be produced during a 1-year period at an average wind speed of 5.0 m/s has been obtained as approximately 384 kWh/year by a Rayleigh wind speed distribution and the power curve.
- The AEP per swept area of our MWT was found to be about 318 kWh/m<sup>2</sup> and the cost of the generated electricity was calculated as 0.32 €/kWh.

Here I would like to draw attention to the fact that the utilization of SWTs has increased in industrialized countries in recent times. The United States, China, and some European Union countries have developed their own SWT standards and set up independent national/international test centers and test areas for SWTs. Taking all of these developments into account, it is necessary that Turkey should determine its own MWT standards; set up national/international SWT test centers, at which can be carried out the power performance, safety, acoustics, and durability tests of SWTs; and define the test fields of the SWTs.

**Nomenclature**

2p	Number of pole pairs	$P_w$	Instantaneous wind power (W)
c	Cost of generated electricity (€/kWh)	$P_t$	Generated power of the MWT (W)
$C_e$	Actual system cost (€)	R	Rotor radius (m)
$C_p$	Power coefficient	$Q_s$	Number of grooves of stator
$E_{kin}$	Kinetic energy (J)	t	Time (h)
E	AEP (years)	T	Lifespan of a MWT (years)
$hw(v)$	Weibull probability distribution function	u	Linear speed of the turbine blades (m/s)
$h_R$	Rayleigh probability distribution function	v	Wind speed (m/s)
I	Current (A)	$V_{OC}$	Open circuit voltage (V)
k	Shape parameter	$\omega_t$	Mechanical angular speed of the MWT blades (rad/s)
$\dot{m}$	Mass flow amount of air (kg/s)	$\lambda$	Tip speed ratio
n	Rotational speed (rpm)	$\rho$	Air density (kg/m <sup>3</sup> )

**Acknowledgment**

The author gratefully acknowledges the support provided for this work by Turgay Mamur. This study would not have been possible without the cooperation and assistance of the institution's personnel.

**References**

- [1] Miranda V. Wind power, distributed generation: new challenges, new solutions. *Turk J Electr Eng Co* 2006; 14: 455–473.
- [2] Dursun B, Gökçol C. Economic analysis of a wind-battery hybrid system: An application for a house in Gebze, Turkey, with moderate wind energy potential. *Turk J Electr Eng Co* 2012; 20: 319–333.
- [3] Akpınar A. Evaluation of wind energy potentiality at coastal locations along the north eastern coasts of Turkey. *Energy* 2013; 50: 395–405.
- [4] Ozgener O. A small wind turbine system (SWTS) application and its performance analysis. *Energy Convers Manage* 2006; 47: 1326–1337.
- [5] Orlando NA, Liserre M, Mastomauro RA, Dell'Aquila A. A survey of control issue in PMSG-based small wind-turbine systems. *IEEE T Ind Inform* 2013; 9: 1211–1221.
- [6] Demirtaş M, Şerefoğlu Ş. Design and implementation of a microcontroller-based wind energy conversion system. *Turk J Electr Eng Co* (in press).
- [7] Tarimer I, Yuzer EO. Designing of a permanent magnet and directly driven synchronous generator for low speed turbines. *Elektron Elektrotech* 2011; 112: 15–18.
- [8] Tarimer I, Ocak O. Performance comparison of internal and external rotor structured wind generators mounted from same permanent magnets on same geometry. *Elektron Elektrotech* 2009; 92: 65–70.
- [9] Bharanikumar R, Kumar AN. Performance analysis of wind turbine-driven permanent magnet generator with matrix converter. *Turk J Electr Eng Co* 2012; 20: 299–317.
- [10] Pyrhönen J, Nerg J, Kurronen P, Puranen J, Haavisto M. Permanent magnet technology in wind power generators. In: 2010 XIX International Conference on Electrical Machines; 6–8 September 2010; Rome, Italy. pp. 1–6.
- [11] Shi J, Chai F, Li X, Cheng S. Study of the number of slots/pole combinations for low speed high torque permanent magnet synchronous motors. In: IEEE 2011 International Conference on Electrical Machines and Systems; 20–23 August 2011; Beijing, China. pp. 1–3.
- [12] Salminen P. Fractional slot permanent magnet synchronous motors for low speed applications. PhD, Lappeenranta University of Technology, Lappeenranta, Finland, 2004.

- [13] Salminen P, Niemelä M, Pyrhönen J, Mantere J. Performance analysis of fractional slot wound PM-motors for low speed applications. In: IEEE 39th IAS Annual Meeting Industry Applications Conference; 3–7 October 2004; Seattle, WA, USA. pp. 1032–1037.
- [14] Cistelecan MV, Popescu M. Study of the number of slots/pole combinations for low speed permanent magnet synchronous generators. In: IEEE International in Electric Machines & Drives Conference; 3–5 May 2007; Antalya, Turkey. pp. 1616–1620.
- [15] Müller G, Jentsch MF, Stoddart E. Vertical axis resistance type wind turbines for use in buildings. *Renew Energ* 2009; 34: 1407–1412.
- [16] Elfarra MA. Horizontal axis wind turbine rotor blade: Winglet and twist aerodynamic design and optimization using CFDV. PhD, Middle East Technical University, Ankara, Turkey, 2011.
- [17] Ozgener O. A review of blade structures of SWTs in the Aegean region and performance analysis. *Renew Sust Energ Rev* 2005; 9: 85–99.
- [18] Pathike P, Katpradit T, Terdtoon P, Sakulchangsatjatai P. A new design of blade for small horizontal-axis wind turbine with low wind speed operation. *Energy Research Journal* 2013; 4: 1–7.
- [19] Rolak M, Kot R, Malinowski M, Goryca Z, Szuster JT. AC/DC converter with maximum power point tracking algorithm for complex solution of small wind turbine. *Prz Elektrotechniczn* 2011; 87: 91–96.
- [20] Selig MS. New airfoils for small horizontal axis wind turbines. *J Sol Energ-T ASME* 1998; 51: 108–114.
- [21] Selig MS, McGranahan BD. Wind tunnel aerodynamic tests of six airfoils for use on small wind turbines; period of performance: October 31, 2002–January 31, 2003. NREL/SR-500-34515. Golden, CO, USA: National Renewable Energy Laboratory, 2004.
- [22] Migliore P, Oerlemans S. Wind tunnel aeroacoustic tests of six airfoils for use on small wind turbines. *J Sol Energ-T ASME* 2004; 126: 974–985.
- [23] Ani SO, Polinder H, Ferreira JA. Comparison of energy yield of small wind turbines in low wind speed areas. *IEEE Transactions on Sustainable Energy* 2013; 4: 42–49.
- [24] Elizondo J, Martinez J, Probst O. Experimental study of a small wind turbine for low- and medium-wind regimes. *Int J Energ Res* 2009; 33: 309–326.
- [25] Whale J, McHenry MP, Malla A. scheduling and conducting power performance testing of a small wind turbine. *Renew Energ* 2013; 55: 55–61.
- [26] Sahin AZ, Al-Garni AZ, Al-Farayedhi A. Analysis of a small horizontal axis wind turbine performance. *Int J Energ Res* 2001; 25: 501–506.
- [27] Bowen A, Huskey A, Link H, Sinclair K, Forsyth T, Jager D, van Dam J, Smith J. Small wind turbine testing results from the National Renewable Energy Lab. In: The International Small Wind Conference; 27–28 April 2010; Glasgow, UK.
- [28] Ata R, Çetin NS. Construction and energy generation of 3 kW autonomous wind turbine. *J Fac Eng Arch Gazi Univ* 2008; 23: 41–47.
- [29] Thapar V, Agnihotri G, Sethi VK. Critical analysis of methods for mathematical modelling of wind turbines. *Renew Energ* 2011; 36: 3166–3177.
- [30] Khezamia N, Braiek NB, Guillaud X. Wind turbine power tracking using an improved multimodel quadratic approach. *ISA T* 2010; 49: 326–334.
- [31] Martinez J, Morales A, Probst O, Llamas A, Rodriguez C. Analysis and simulation of a wind-electric battery charging system. *Int J Energ Res* 2006; 30: 633–646.
- [32] Celik AN. A statistical analysis of wind power density based on the Weibull and Rayleigh models at the southern region of Turkey. *Renew Energ* 2003; 29: 593–604.
- [33] Kishore RA, Coudron T, Priya S. Small-scale wind energy portable turbine (SWEPT). *J Wind Eng Ind Aerod* 2013; 116: 21–31.